



# Design and implementation of a BDS precise point positioning service

Cheng Liu<sup>1</sup>  | Weiguang Gao<sup>1</sup> | Tianxiong Liu<sup>2</sup> | Dun Wang<sup>3</sup> | Zheng Yao<sup>4</sup>  | Yang Gao<sup>5</sup> | Xin Nie<sup>2</sup> | Wei Wang<sup>1</sup> | Dongjun Li<sup>3</sup> | Weixing Zhang<sup>6</sup> | Dongxia Wang<sup>5</sup> | Yongnan Rao<sup>7</sup>

<sup>1</sup> Beijing Institute of Tracking and Telecommunication Technology, Beijing, China

<sup>2</sup> Beijing Institute of Spacecraft System Engineering, Beijing, China

<sup>3</sup> Space Star Technology Co., Ltd, Beijing, China

<sup>4</sup> Department of Electronic Engineering, Tsinghua University, Beijing, China

<sup>5</sup> Beijing Navigation Center, Beijing, China

<sup>6</sup> GNSS Research Center, Wuhan University, Beijing, China

<sup>7</sup> National Time Service Center, Chinese Academy of Sciences, Xi'an, China

## Correspondence

Cheng Liu, Beijing Institute of Tracking and Telecommunication Technology, Beijing, China.

Email: [liucheng@beidou.gov.cn](mailto:liucheng@beidou.gov.cn)

## Funding information

National Natural Science Foundation of China, Grant/Award Numbers: 41974041, 61601009, 61771272; China Association for Science and Technology, Grant/Award Number: 2019QNRC001

## Abstract

Precise point positioning (PPP) service is of great significance for BDS. The design and implementation of the service are presented. The PPP-B2b signal of the service is constructed, which is efficient multiplexed with other signal components, and achieves compatibility between two service phases. A customized message format that can augment all visible satellites of four core constellations in mainland China is proposed. The high-gain, 64-ary, low-density parity check (LDPC) coding is used, which facilitates the integrated design of the receivers. A signal quality test has revealed that the S-curve bias (SCB) of PPP-B2b does not exceed 0.0165 ns and the coherence between the code and the carrier of the signal is only 0.137°. A performance evaluation has indicated that at its current stage, the positioning accuracy in the horizontal and vertical directions is better than 0.15 m and 0.3 m, respectively, and the convergence time does not exceed 800 s.

## KEYWORDS

ACE-BOC, B2b, BeiDou, LDPC, PPP, SSR

## 1 | INTRODUCTION

Precise point positioning (PPP) is an important technology for achieving wide area high-precision positioning for a satellite navigation system because of its wide signal coverage, uniform accuracy distribution, and small number of ground reference monitoring stations (Héroux & Kouba, 2001). With the technical and capability improvements of

satellite navigation systems in recent years, it has become a trend to provide embedded PPP services based on basic navigation constellations.

Galileo is designed to provide a global “free of charge high-precision PPP service” via its E6B signal with an expected accuracy of 20 cm and a broadcast data rate of 500 bps. Currently, the interface control document (ICD) of the service is “under final consolidation” (Hayes, 2018;

Hayes & Hahn, 2019). QZSS provides its centimeter-level augmentation service (CLAS), which covers Japan, based on real-time kinematic precise point positioning (PPP-RTK) technology via its L6D signal. As stated in the QZSS performance standard (PS) and interface specification document (IS-QZSS-L6-001) released in November 2018, the CLAS broadcast data rate reaches 2,000 bps and can achieve centimeter-level accuracy in one minute (Cabinet Office, 2018a, 2018b). In addition, QZSS is conducting technology validation of a wide centimeter-level augmentation service that can cover the Asia-Pacific region via the L6E signal of QZS-2 to QZS-4 (QZSS, 2018). GLONASS also announced its “high-precision service, navigation in absolute regime using phase measurements (PPP) on a commercial basis” with an expected accuracy of 0.1 m, which will mainly be applied in precision engineering, emergency road service (ERS), unmanned transport, etc. (Revnivkykh, 2019).

The BeiDou global navigation satellite system (BDS-3) attaches great importance to the construction and development of the PPP service. On December 27, 2019, the BDS-3 held a press conference to mark the first anniversary of its global services and announced seven kinds of services, including PPP (Office China Satellite Navigation, 2019a, 2019b). At the same time, PPP service-related documents such as The Application Service Architecture of BeiDou Navigation Satellite System (Version 1.0) and the Space Interface Control Document Open Service Signal PPP-B2b (Beta Version) were officially released. The BDS PPP service uses the B2b signal of the BDS-3 geostationary earth orbit (GEO) satellites (i.e., PPP-B2b) as a data broadcast channel. Its construction includes two phases (Office China Satellite Navigation, 2019b, 2019c). In the first phase (until 2020), the PPP-B2b I-components (PPP-B2b\_I) of the first three GEO satellites are used to provide a free and high-precision service for users in China and surrounding areas. In the second phase (after 2020), with the launch of subsequent satellites, the service will expand its coverage, further improve the accuracy, reduce the convergence time, and better serve high-precision application fields such as land surveying, precision agriculture, and marine development.

This study focuses on the design and implementation of the BDS PPP service, which is integrated with BDS-3 and works by using the space and ground segment facilities of BDS-3. To make better use of the GEO satellites and achieve compatibility with other BDS services and the successive PPP service in the different phases, the PPP-B2b signal of the service is constructed based on the optimized asymmetric constant envelope binary offset carrier (ACE-BOC) multiplexing modulation method (Yao et al., 2016). By studying the factors influencing the PPP augmentation navigation message, the customized compression message

format of the service is formulated, which can augment all visible satellites of the four core constellations (GPS, GLONASS, BDS, and Galileo) in mainland China. The same high-gain, 64-ary, low-density parity check (LDPC) coding (Huang et al., 2017, 2019) for navigation messages used in the B2b signal of the medium earth orbit (MEO) and inclined geosynchronous orbit (IGSO) satellites is also used for the PPP service, which facilitates the integrated design of the receivers. The signal quality testing and positioning performance evaluation works are also performed and presented, which prove the effectiveness of the design and indicate that the service, at its current stage of development, has satisfactory capabilities.

The remainder of this paper is structured as follows. Section 2 presents the architecture and data processing flow of the service. Section 3 illustrates the scheme design of PPP-B2b. Section 4 studies the key to the augmentation navigation messages and briefly introduces the customized optimization message format of the BDS PPP service. The 64-ary LDPC coding and its actual receiving testing results, which prove its high gain and effectiveness, are provided in Section 5. Finally, Section 6 presents the signal quality testing results of PPP-B2b broadcast by GEO-1 in orbit and describes the initial performance evaluation results of the service.

## 2 | BDS PPP SERVICE SYSTEM

This section presents the basic composition of the BDS PPP service system, which is integrated with BDS-3, including its system architecture and data processing flow.

### 2.1 | System architecture

As part of BDS-3, the BDS PPP service works by using the space and ground segment facilities of BDS-3. The space segment of the service currently includes three BDS-3 GEO satellites that operate in orbit at an altitude of 35,786 km and are located at longitudes 80°, 110.5°, and 140°. The coverage areas of the three GEO satellites are shown in Figure 1, in which the coverage areas corresponding to a 0° elevation angle are indicated by oval colors and those corresponding to the 5° and 10° elevation angle are marked with oval lines. The B2b signals of the BDS-3 GEO satellites used for the PPP message broadcast are called “PPP-B2b.” The first two BDS-3 GEO satellites (GEO-1 and GEO-2) were launched in November 2018 and April 2020, respectively, and the last one (GEO-3) will be launched in the first half of 2020. These three satellites provide the first-phase service. In the future, more BDS-3 GEO satellites

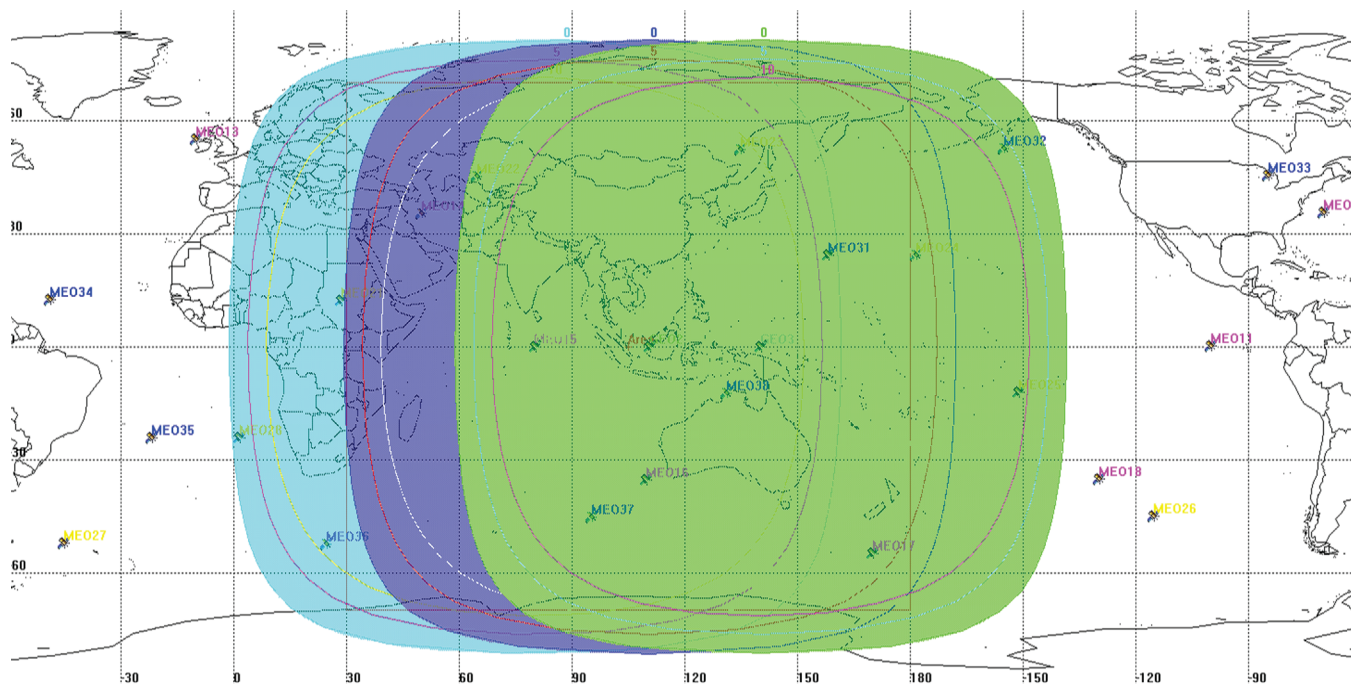


FIGURE 1 Signal coverage of BDS-3 GEOs [Color figure can be viewed in the online issue, which is available at wileyonlinelibrary.com and www.ion.org]

for backup will be launched to provide the second-phase service.

The ground segment consists of the master control station (MCS), uplink stations (ULS), and monitoring stations (MS), which are well distributed in mainland China and have better geometry than that of the BeiDou regional navigation satellite system (BDS-2) (Yang et al., 2019). The MCS, ULS, and MS are shared with other BDS-3 open services.

The user segment includes various receivers with PPP-B2b signal reception, augmentation navigation message demodulation, and PPP solution functions, which are mainly applied in fields such as precision agriculture, advanced driver assistance system (ADAS), and marine development.

## 2.2 | Data processing flow

The data processing flow of the service is shown in Figure 2. The MS carries out continuous monitoring for all the visible satellites of the global navigation satellite systems (GNSS), forming pseudorange and carrier phase observations, and collecting meteorological data. After pre-processing, the raw data are sent to the MCS via a network.

The quality verification and accuracy assessment for the raw data are carried out by the MCS for pre-processing.

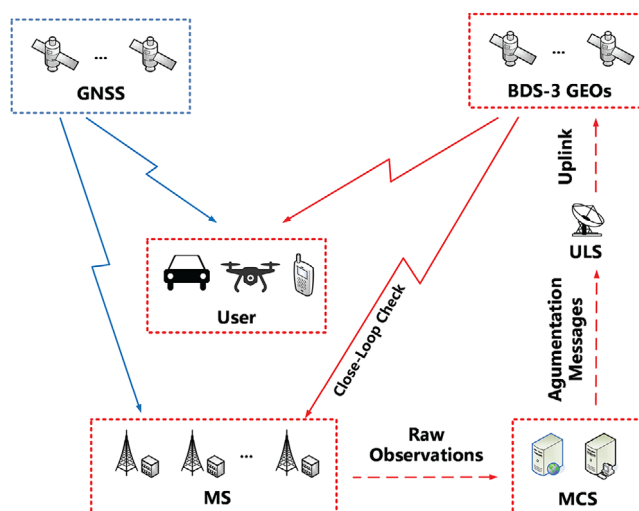


FIGURE 2 Data processing flow of BDS PPP service [Color figure can be viewed in the online issue, which is available at wileyonlinelibrary.com and www.ion.org]

The raw data are compared with historical precise products for the overlapping arcs, and the user differential range error (UDRE) is evaluated. After pre-processing, the precise prediction satellite orbit and clock corrections are solved and fitted based on a dynamical smoothing process (Hadas & Bosy, 2014; Kazmierski et al., 2017). According to the design protocol and format, the corrections and other related parameters such as mask and differential code bias

(DCB) are attached to the augmentation navigation messages and then transferred to the ULS.

The ULS transmits the augmentation navigation messages to the GEO satellites for broadcasting via PPP-B2b signals. Meanwhile, the MS and MCS retrieve the messages for closed-loop checking.

### 3 | SIGNAL SCHEME DESIGN

The BDS PPP service is based on the BDS-3 GEO satellites and is limited by the actual transmitting power of the satellites and other conditions; furthermore, it needs to consider the compatibility and succession of different service phases. These requirements pose challenges to the design of the PPP-B2b signal scheme. This section mainly introduces a demonstration of the PPP-B2b signal and the design work undertaken to realize it.

#### 3.1 | Downlink calculation

The B2 band of the BDS-3 GEO satellites includes two signals, B2a and B2b (i.e., PPP-B2b). B2a provides a dual-frequency, multi-constellation (DFMC), satellite-based augmentation system (SBAS) service (known as the “BDSBAS-B2a” signal), which must meet the minimum received radiated power requirement ( $-158.5$  dBW) of the SBAS Interoperability Working Group (SBAS IWG) and the International Civil Aviation Organization (ICAO) (IWG SBAS, 2016a, 2016b; ICAO, 2018). Therefore, PPP-B2b must perform a signal scheme design that does not affect the DFMC SBAS service on BDSBAS-B2a.

The design maximum effective isotropic radiated power (EIRP) of the first three BDS-3 GEO satellites at the B2 band is 34 dBW. The power distribution between BDSBAS-B2a and PPP-B2b is at a ratio of 2:1 to ensure that the received power of BDSBAS-B2a meets the international standard. Further, considering the constant envelope efficiency loss of BDSBAS-B2a and PPP-B2b multiplexing, the EIRP of PPP-B2b does not exceed 28.4 dBW, which translates to a ground received power of  $-159.5$  dBW, corresponding to an elevation angle of  $5^\circ$ .

In terms of terminal reception, the B2 signal reception performances of various products from a few GNSS receiver manufacturers in China were investigated, including the vehicle, geodetic, and handheld categories of receivers. In addition, considering the increasing popularity of GNSS high-precision applications, the portable, miniaturized category of receivers was also investigated. The sensitivity indicator of the receivers is usually expressed by the G/T value, where “G” is the gain of the receiving antenna and “T” is the equivalent noise tem-

perature of the receivers. By averaging the G/T values of the different categories of receivers of the above manufactures, typical G/T values were obtained, as shown in Table 1.

Considering actual application in multiple environments, a certain demodulation margin is necessary for reliable use. Taking the typical G/T value of a  $5^\circ$  elevation angle as the critical G/T value, the downlink of PPP-B2b can be calculated based on the satellite EIRP and the space transmission loss. As shown in Table 2, it can support the reception of various receivers with a data rate of 500 bps, including some miniaturization terminals with low G/T values.

#### 3.2 | Modulation and structure

The PPP-B2b of the first-phase service adopts binary phase shift keying (BPSK) (10) modulation for the following reasons. First, the message frame corresponding to BPSK includes only one preamble and cyclic redundancy check (CRC), which saves more useful bits than the quadrature phase shift keying (QPSK) modulation. Second, it achieves backward and forward compatibility and succession between the two service phases. Specifically, the first-phase service of the BDS PPP can be realized through the I-components of the first three GEO satellites (PPP-B2b\_I). With the modulation and data rate of PPP-B2b\_I unchanged, the added data rate and message content for the second-phase service can be realized via the Q-components of the subsequent GEO satellites (PPP-B2b\_Q); thus, PPP-B2b\_I on all GEO satellites are the same for users. Finally, BPSK (10) modulation also enables PPP-B2b\_I to adopt both the ranging codes with the same features and the identical coding method used in the B2b signal of the MEO and IGSO satellites (Office China Satellite Navigation, 2019d), which facilitates integrated design of the BDS receivers. The modulation and structure of PPP-B2b are shown in Table 3.

#### 3.3 | Multiplexing signal based on Type-III ACE-BOC modulation

As described in Sections 3.1 and 3.2, the PPP-B2b signals of the first three GEO satellites retain only the I-component. The power ratio of the PPP-B2b\_I, BDSBAS-B2a I-component (i.e., BDSBAS-B2a\_I), and BDSBAS-B2a Q-component (i.e., BDSBAS-B2a\_Q) was 1:1:1.

The flexibility of ACE-BOC, especially in terms of the number of involved components and their power allocations, makes it a good solution for many special scenarios



TABLE 1 Typical G/T of receivers\*

Performance	Receiver Type				Elevation Angle (°)
	Vehicle	Geodetic	Hand-held	Portable	
Typical G/T (dB/K)	$\leq -30.7$	$\leq -32.7$	$\leq -32.7$	$\leq -33.9$	5
	$-26.2 \sim -28.6$	$-26.7 \sim -30.0$	$-28.6 \sim -34.0$	$\leq -30.0$	20
	$-22.7 \sim -25.1$	$-22.7 \sim -24.1$	$-24.7 \sim -25.1$	$-26.1 \sim -26.4$	50
	$-20.7 \sim -21.1$	$-19.6 \sim -20.7$	$-21.0 \sim -25.0$	$-23.4 \sim -25.6$	90

\*The G/T values of the receivers are tested and provided by the manufacturers. Because of the limited number of manufacturers surveyed and the performance and test conditions of the receivers are also different, the typical G/T values in the table are only presented as reference.

TABLE 2 Downlink calculation of PPP-B2b

Items	Values			
Maximum ERIP of PPP-B2b (dBW)	28.4			
Spatial transmission loss of L-band (dB)	-186.4			
Antenna polarization and pointing loss (dB)	-1.5			
Ground received signal power (dBW)	-159.5			
Broadcast data rate (bps)	500			
$C/N_0$ threshold with BER less than $10^{-6}$ (dBHz)	37.6			
Designed coding gain (dB)	7.5			
A/D conversion and baseband processing loss (dB)	2			
	Vehicle	Geodetic	Hand-held	Portable
Typical G/T of receivers (dB/K)	-30.7	-32.7	-32.7	-33.9
Effective $C/N_0$ (dB-Hz)	38.3	36.3	36.3	35.1
Demodulation margin (dB)	6.3	4.3	4.3	3.1

satisfying the requirements of modern GNSS signal structure design. When the power ratio of PPP-B2b, BDSBAS-B2a\_I, and BDSBAS-B2a\_Q is 1:1:1, the signal multiplexing scheme corresponds to the Type-III ACE-BOC modulation.

However, Type-III ACE-BOC modulation is susceptible to the effects of the intermodulation components. On one hand, when the relative phase between PPP-B2b\_I and BDSBAS-B2a\_I is  $0^\circ$ , the intermodulation components introduced to maintain the constant envelope of the composite B2 signal are relatively large, thereby reducing the multiplexing efficiency (the ratio of the total actual power of the composite signal to the total transmission power of the satellite). On the other hand, the intermodulation components will interfere with the useful components and increase the DCBs between components.

To solve the problem mentioned above, a “phase rotation” operation on PPP-B2b\_I is performed, so that

its relative phase with respect to BDSBAS-B2a\_I and BDSBAS-B2a\_Q changes from  $0^\circ$  to  $45^\circ$ , as shown in Figure 3. Furthermore, the constant envelope multiplexing intermodulation construction (CEMIC) method is used to optimize the multiplexing signal with the power and phase constraints mentioned above and to suppress the intermodulation components by forcibly setting their weighting coefficients to zero (Yao et al., 2017). Finally, the multiplexing signals of BDSBAS-B2a and PPP-B2b based on the optimized Type-III ACE-BOC modulation are constructed.

The actual power and multiplexing efficiency of the composite B2 signal based on the optimized Type-III ACE-BOC modulation are shown in Table 4, and the corresponding constellation and power spectral density with the unlimited bandwidth are shown in Figures 4 and 5, respectively. As shown in Figure 4, the optimized Type-III ACE-BOC modulation maintains a constant envelope of the

TABLE 3 Modulation and structure of PPP-B2b

Signal	Component	Carrier frequency (MHz)	Modulation	Symbol rate (sps)	First three GEOs	Subsequent GEOs
PPP-B2b	I	1207.14	BPSK (10)	1000	available	available
	Q	1207.14	TBD	TBD	N/A	available

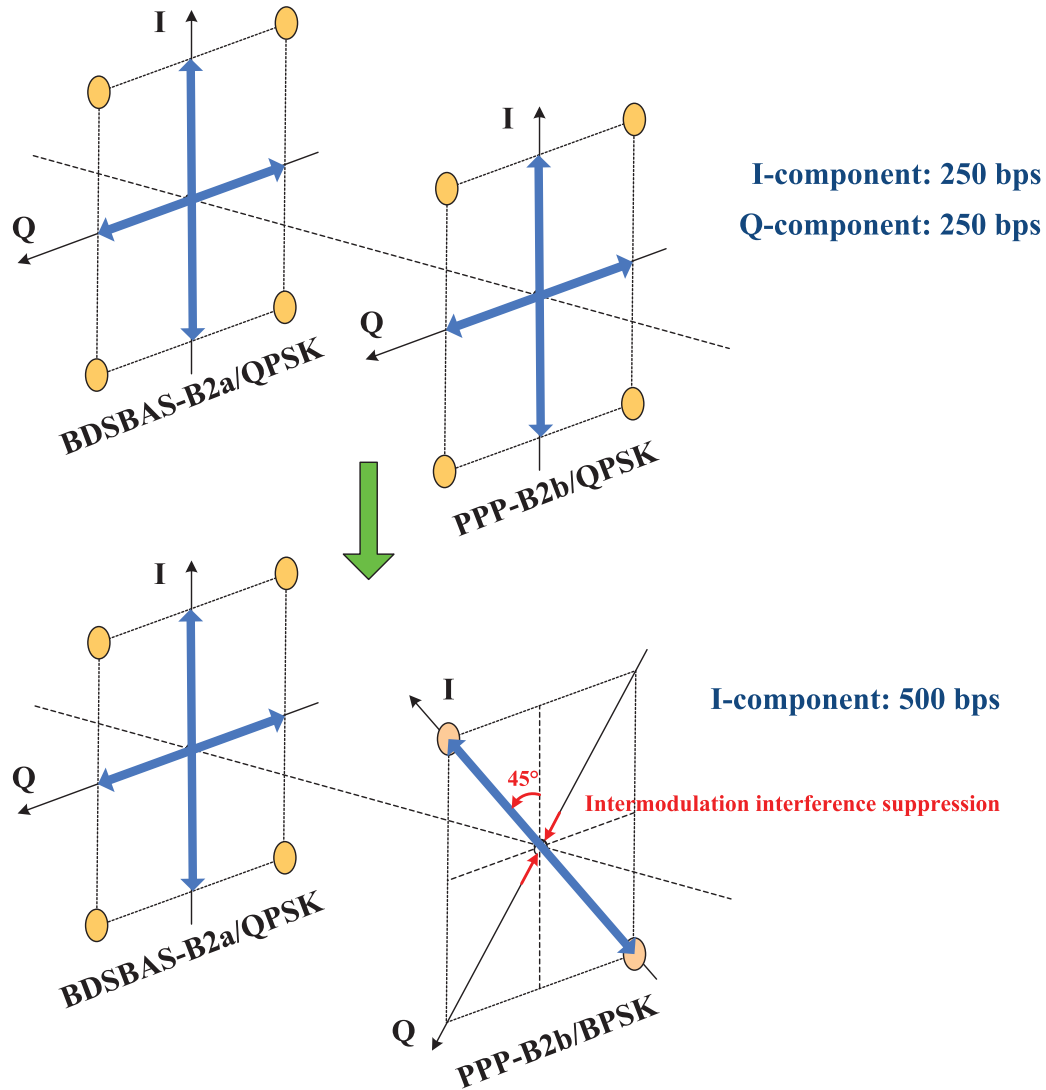


FIGURE 3 Phase rotation of PPP-B2b\_I [Color figure can be viewed in the online issue, which is available at wileyonlinelibrary.com and www.ion.org]

TABLE 4 Power and multiplexing efficiency corresponding to the optimized Type-III ACE-BOC

Power ratio of B2a-I:B2a-Q: B2b-I:B2b-Q	Actual power*				Multiplexing efficiency	Phase relationship between B2b-I and B2a-I	
	Signal components	B2a-I	B2a-Q	B2b-I			B2b-Q
1:1:1:0	Unlimited bandwidth	0.2374	0.2374	0.2374	0	71.22%	45°
	Working bandwidth	0.3118	0.3118	0.3118		93.54%	

\*The total transmission power is assumed to be 1.

signal, and it can be seen from Table 4 and Figure 5 that the cost of suppressing the effect of the intermodulation components is the loss of a certain amount of actual power and multiplexing efficiency of the signal. With the unlimited bandwidth, the multiplexing efficiency of the composite B2 signal was 71.22%. However, it should be noted that the intermodulation components in the multiplexing signal mainly exist at the higher harmonics of the subcarrier

(see Figure 5). As the actual transmission bandwidth of B2 is 71.61 MHz, after filtering by the onboard filter, the proportion of the intermodulation component in the actual transmission signal is significantly reduced to only 6.46% of the total power. In other words, the multiplexing efficiency of the signal with the actual transmission bandwidth can reach 93.54%, which indicates an ideal signal scheme design.

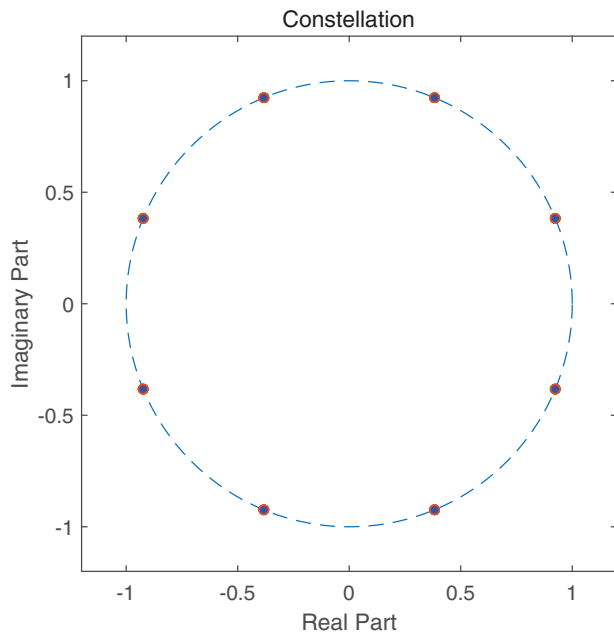


**FIGURE 4** Constellation corresponding to optimized Type-III ACE-BOC [Color figure can be viewed in the online issue, which is available at [wileyonlinelibrary.com](http://wileyonlinelibrary.com) and [www.ion.org](http://www.ion.org)]

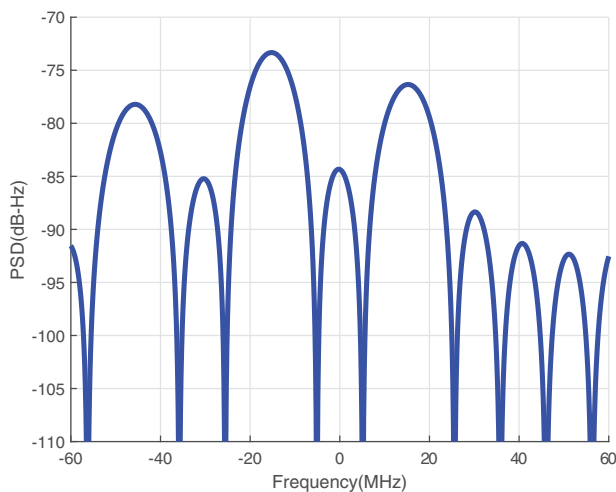


**FIGURE 5** PSD corresponding to optimized Type-III ACE-BOC [Color figure can be viewed in the online issue, which is available at [wileyonlinelibrary.com](http://wileyonlinelibrary.com) and [www.ion.org](http://www.ion.org)]

Note that the phase rotation operation only changes the relative phase relationship between BDSBAS-B2a and PPP-B2b, but not the phase relationship between different components of the same signal. Thus, it has no effect on receivers that receive PPP-B2b individually. Furthermore, the addition of the PPP-B2b<sub>Q</sub> component on subsequent GEO satellites will not affect the operation of receivers and their ability to receive PPP-B2b<sub>I</sub>. This is another advantage of the multiplexing signal.

## 4 | MESSAGE FORMAT DESIGN

As the construction and development of PPP systems or services in the world were initially commercial activities, and the satellite link resources used were different, they did not formulate a unified and standard augmentation message format like SBAS. Generally, each PPP system or service customizes its own augmentation message format based on its actual broadcast link resource conditions and service performance requirements. This section introduces the design of the augmentation message format of the BDS PPP service and summarizes its characteristics.

### 4.1 | Design factors

Because the bandwidth of the satellites used for broadcasting is limited and valuable, an optimized design of the navigation message format is necessary. For the PPP augmentation navigation message format, the number of augmented satellites, the bit length, and the update interval of the satellite corrections are important design factors.

#### 4.1.1 | Augmented satellites number

The number of satellites that need to be augmented is an important prerequisite for the design of the PPP service message format. Based on the number of augmented satellites, the approximate amount of correction data bits can be estimated to better carry out the subsequent design.

The first phase of the BDS PPP service uses PPP-B2b<sub>I</sub> to provide services for users in China and its surrounding areas. Therefore, a simulation of each GNSS's visibility in mainland China was performed to obtain the maximum numbers of visible satellites with different GNSS combinations, as shown in Table 5. It can be seen that, for the regional service of the first phase, to achieve the augmentation of the four core GNSS constellations, information such as the orbit and clock corrections of 68 satellites should be broadcast. This activity is no small task for satellite broadcasting. Therefore, to avoid loss of correction accuracy (referred to as “correction accuracy loss” in this paper) caused by the large update interval of the satellite corrections, the BDS PPP service should compress and optimize the augmentation message format.

#### 4.1.2 | Correction bit length

The compression of the message is mainly determined by the bit length of the corrections (referred to as “correction bit length” in this paper), which is jointly determined by

TABLE 5 Maximum number of visible satellites in mainland China under different GNSS combinations

GNSS combination	BDS	BDS+GPS	BDS+GPS+GLO	BDS+GPS+GLO+GAL
Maximum number of visible satellites	20	36	49	68

TABLE 6 Correction bit Length of the BDS PPP service

Correction	Standard SSR			BDSBAS PPP service		
	Length (bit)	Scale factor	Range	Length (bit)	Scale factor	Range
Orbit correction (R)	22	0.1 mm	±209.7151 m	15	1.6 mm	±26.2128 m
Orbit correction (A)	20	0.4 mm	±209.7148 m	13	6.4 mm	±26.208 m
Orbit correction (C)	20	0.4 mm	±209.7148 m	13	6.4 mm	±26.208 m
Clock correction ( $C_0$ )	22	0.1 mm	±209.7151 m	15	1.6 mm	±26.2128 m
Clock correction ( $C_1$ )	21	0.001 mm/s	±1.048575 m/s	–	–	–
Clock correction ( $C_2$ )	27	0.00002 mm/s <sup>2</sup>	±1.342177 m/s <sup>2</sup>	–	–	–
Differential code bias	14	0.01 m	±81.91 m	12	0.02 m	±35.746 m
URA	6	1	0~7	6	1	0~7

the value range and scale factor of the corrections. The value range determines the upper and lower limits of the corrections; that is, an excessively large value range will waste the bits, and a small value range will cause truncation error. The scale factor determines the resolution of the described corrections in that an excessively large scale factor will lead to a precision reduction of the corrections; if it is too small, substantial bits will be occupied in the same value range. Thus, the design of the correction bit length should consider the impact of both the performance and the bit resource. We denote the correction bit length and the scale factor as  $n$  (unit: bits) and  $m$  (unit: m), respectively; then the valid representation range  $R$  of the correction is

$$-2^{n-1} \cdot m \leq R \leq +2^{n-1} \cdot m. \quad (1)$$

Compared to the standard state space representation (SSR) format formulated by the Radio Technical Commission for Maritime Services (RTCM) (RTCM Special Committee, NO.104 18, 2013), the BDS PPP service greatly compresses the bit length of the parameters such as the satellite orbit correction, clock correction, DCB, and user range accuracy (URA) (please see Table 6 for details). By compressing the correction bit length, more satellites can be augmented by using the same bit resource or at the same broadcast rate. With the same number of augmented satellites, the service can have smaller correction update intervals, thereby reducing the accuracy loss of the corrections.

The satellite orbit and clock error and signal-in-space range error (SISRE) can be evaluated by comparing the

broadcast ephemeris with the precise ephemeris. This study used the GNSS broadcast ephemeris for 31 days in January 2017 and the precise orbit and clock products of multi-GNSS (GBM) released by the Helmholtz-Centre Potsdam-German Research Centre for Geosciences (GFZ) as a reference to obtain the orbit and clock corrections of GNSS satellites (1 s for sampling). The probabilities of the orbit and clock corrections falling within the range of the standard SSR format and the BDS PPP service message format were calculated, respectively, as shown in Table 7.

According to Table 7, the BDS PPP service message format greatly compresses the correction bit length compared to the standard SSR; however, it still guarantees that the probabilities of the GNSS satellite orbit and clock corrections falling within the design value ranges are greater than 99.9%, which will not affect the performance of the service.

#### 4.1.3 | Correction update interval

Similar to the basic broadcast message of a satellite navigation system, the PPP augmentation navigation message is generally composed of multiple message types, and the satellite orbit corrections, clock corrections, and other related parameters are cyclically broadcast in the corresponding message types. Therefore, the user will receive the updated corrections of a certain navigation satellite in a certain period, which is the update interval of the corrections.

At the current time  $t$ , the user can only use the historical corrections of the previous reference time  $t_0$  for



**TABLE 7** Probabilities of corrections falling within the ranges of different message formats

GNSS	Message format	Orbit correction (%)			Clock correction (%)	Differential code bias (%)
		Radial	Cross	Along		
BDS	Standard SSR	100.00	99.99	100.00	100.00	100.00
	BDS PPP Service	99.94	99.98	99.94	99.93	100.00
GPS	Standard SSR	100.00	99.99	99.99	100.00	100.00
	BDS PPP Service	100.00	99.99	99.99	100.00	100.00
GLO	Standard SSR	99.99	99.99	99.99	100.00	100.00
	BDS PPP Service	99.99	99.99	99.99	100.00	100.00
GAL	Standard SSR	100.00	100.00	100.00	100.00	100.00
	BDS PPP Service	100.00	99.94	99.99	99.99	100.00

**TABLE 8** Accuracy loss of GNSS corrections (95%)

Correction	Update interval/s	BDS/m	GPS/m	GLO/m	GAL/m
Orbit correction (R)	30	0.002	0.002	0.014	0.001
	60	0.004	0.004	0.029	0.001
	120	0.007	0.007	0.062	0.002
Orbit correction (C)	30	0.011	0.006	0.015	0.001
	60	0.023	0.012	0.030	0.003
	120	0.046	0.025	0.063	0.005
Orbit correction (A)	30	0.012	0.004	0.014	0.001
	60	0.025	0.009	0.029	0.002
	120	0.050	0.018	0.062	0.004
Clock correction ( $C_0$ )	5	0.002	0.004	0.005	0.000
	10	0.004	0.008	0.009	0.001
	20	0.007	0.017	0.018	0.001

calculations before receiving the new corrections. Thus, the actual accuracy of the corrections used is inversely proportional to the delay time ( $t - t_0$ ). A shorter update interval results in a shorter receiving delay and higher accuracy of the corrections, and vice versa. The accuracy loss of the orbit corrections is mainly related to the satellite orbit motion characteristics, and the accuracy loss of the clock corrections is related to the satellite atomic clock frequency stability (mainly short stability).

To analyze the effect of the update interval on the corrections' accuracy loss, the above-mentioned data were used in a simulation. For each satellite of a GNSS constellation, the accuracy loss of its orbit corrections and clock corrections were calculated, with update intervals from 1 s to 179 s in each 180 s period. Then, the average value of each 180 s period was calculated to obtain the average accuracy loss of each satellite, with update intervals from 1 s to 179 s. Finally, the value of each satellite of the same GNSS was averaged to obtain the accuracy loss of each constellation, as shown in Table 8.

Based on the analysis above, the final impact of the correction update interval on the positioning accuracy was further simulated and evaluated, as shown in Figure 6. It can be seen from Figure 6 that the correction update interval has the least impact on Galileo, followed by BDS and GPS, and has the greatest impact on GLONASS. To achieve a satisfactory positioning accuracy, the design orbit correction update interval was tens of seconds (generally no more than 96 s), and the design clock correction update interval was several seconds (generally no more than 12 s).

## 4.2 | Message structure and content

Considering the key factors mentioned above, to make better use of the satellite downlink bandwidth, the BDS PPP service carried out a compression design based on the standard SSR and developed its customized message format. Thus, PPP-B2b\_I can augment all visible satellites of the four core GNSSs in mainland China with a data frame length of 486 bits.

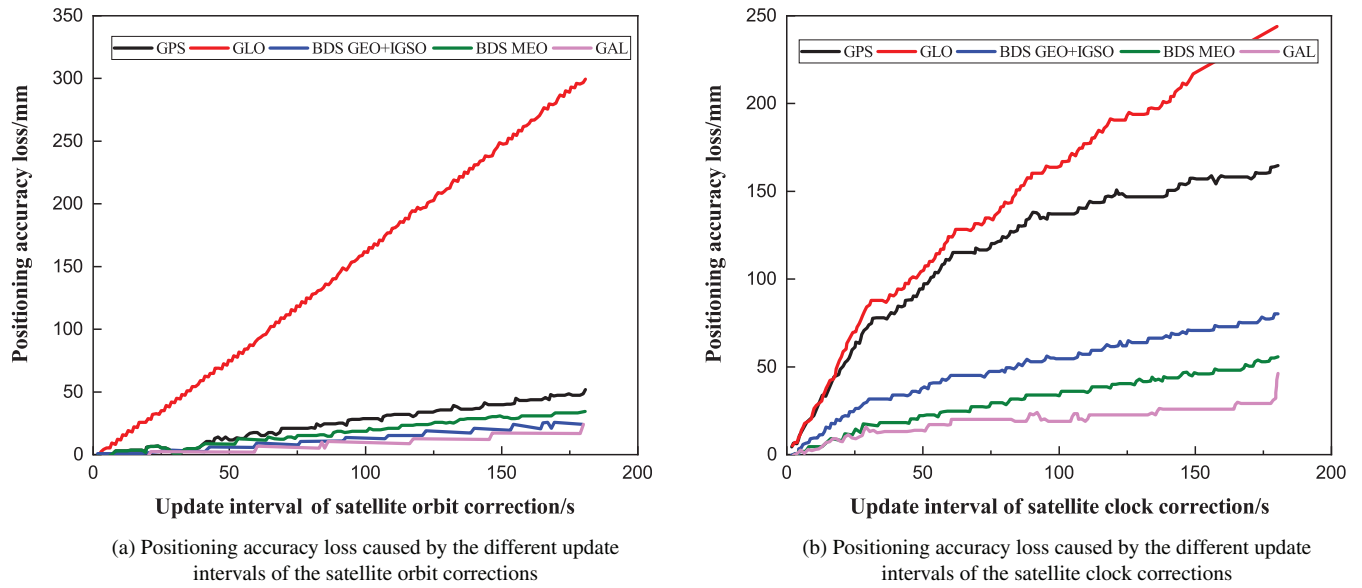
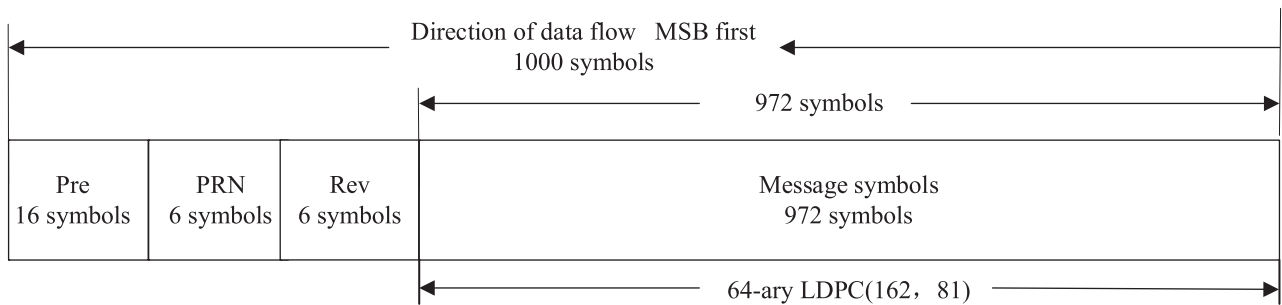


FIGURE 6 Positioning accuracy loss caused by the different update intervals of the satellite corrections [Color figure can be viewed in the online issue, which is available at wileyonlinelibrary.com and www.ion.org]

After error correction encoding:



Before error correction encoding:

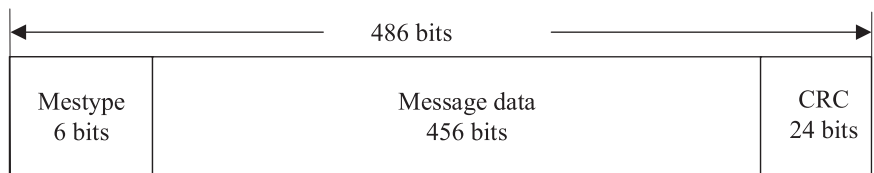


FIGURE 7 PPP-B2b\_I navigation message frame structure

4.2.1 | Message structure

The basic frame structure of the PPP-B2b\_I augmentation navigation message is defined in Figure 7 (Office China Satellite Navigation, 2019c).

Each data frame of the messages has 486 bits, wherein the highest 6 bits indicate the message type, the lowest 24 bits are CRC, and the remaining 456 bits are the message data and its specific contents may vary depending on different message types.

After encoding (see Section 5), the frame length is 972 symbols. These symbols are concatenated together with 16 symbols of the preamble, 6 symbols of the pseudo random noise (PRN) code, and 6 symbols of the reserved flags to form 1,000 symbols in total. The leading edge of the first symbol of each frame should be coincident with the start of the BeiDou navigation satellite system time (BDT) second, and the transmission of each frame will last 1 s.

The reserved flags are used to identify the status of the service: “1” in the highest bit of the reserved flags means the PPP service of this satellite is unavailable, and “0” means that it is available. Other symbols are reserved for future purposes. The status of the reserved flags rarely changes so that users can minimize the demodulation error by superimposing multiple frames of information.

#### 4.2.2 | Message types and content

Based on the analysis in Section 4.1, the BDS PPP service carried out a compression and optimization design of the message types and contents, which includes the following:

1. Using masks to identify a GNSS and its satellites so that each message type can share a common set of satellite masks defined in advance, thereby saving the message bits.
2. Deleting the higher-order terms in the satellite orbit and clock corrections and streamlining the message contents.
3. Compressing the bit length of the satellite orbit and clock corrections, DCBs, and fields, such as epochs, thereby improving the utilization efficiency of message bits.
4. Using message types that broadcast orbit corrections and clock corrections in combination, therefore eliminating the need of large amounts of empty data to supplement the corrections in filling all the data bits of the message.

Seven valid message types have been defined so far, and their nominal validity times are listed in Table 9. The actual update interval of each message type will be shorter than its nominal validity time, but it may change owing to the performance improvement or the number of augmented GNSSs.

## 5 | CODING METHOD DESIGN

As mentioned in Section 3.2, PPP-B2b adopts the same coding method for navigation messages used in the B2b signal of the MEO and IGSO satellites, which is the 64-ary LDPC (Huang et al., 2017, 2019). Based on the system link and the bit error rate (BER) equation, this section analyzes the theoretical gain requirements of various terminals for a 64-ary LDPC. An actual receiving test is then performed and presented in Figure 8, which proves its high gain and effectiveness.

TABLE 9 Defined message types and their nominal validity times

Message type (in decimal)	Information content	Nominal validity time (s)
1	Satellite mask	–
2	Satellite orbit correction and URA	96
3	DCB	86400
4	Satellite clock correction	12
5	URA	96
6	Clock correction and orbit correction - combination 1	96
7	Clock correction and orbit correction - combination 2	96
8–61	Reserved	–
62	Reserved	–
63	Null message	–

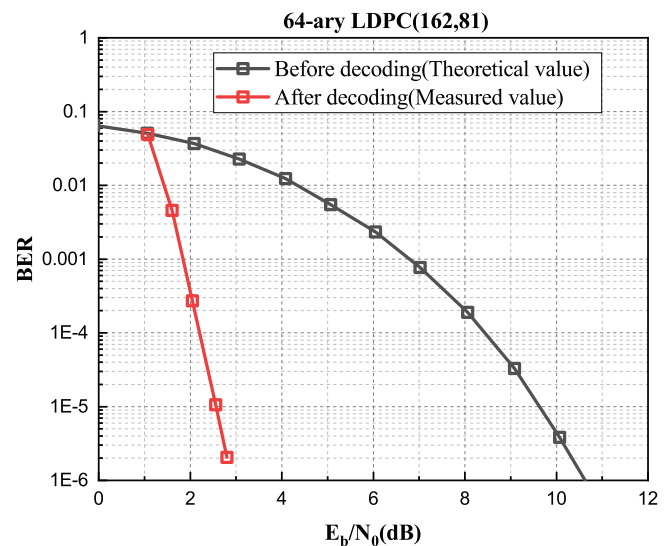


FIGURE 8 Test performance of LDPC(162,81) code [Color figure can be viewed in the online issue, which is available at wileyonlinelibrary.com and www.ion.org]

### 5.1 | Coding gain requirements

The BER ( $P_e$ ) is an important quality indicator of communication systems. The relationship between  $P_e$  and  $E_b/N_0$  (ratio of signal energy to noise power spectral density per bit) is expressed as

$$P_e = \frac{1}{2} \operatorname{erfc}(E_b/N_0)^{1/2}. \quad (2)$$

TABLE 10 Values of  $P_e$ ,  $C/N_0$  and  $E_b/N_0$  ( $T_b = 500$  bps)

Items	Values*							
$C/N_0$ (dB)	36.4	36.6	36.8	37.0	37.2	37.4	37.6	37.8
$E_b/N_0$ (dB)	9.41	9.61	9.81	10.01	10.21	10.41	10.61	10.81
$P_e$	$1.47^{-5}$	$9.55^{-6}$	$6.10^{-6}$	$3.78^{-6}$	$2.32^{-6}$	$1.38^{-6}$	$8.05^{-7}$	$4.58^{-7}$

\*  $a^b$  means  $a \times 10^b$ .

TABLE 11 Coding gain requirements

Items	Values			
Data rate (bps)	500			
Ground received signal power (dBW)	−159.5			
$C/N_0$ threshold with BER less than $10^{-6}$ (dB)	37.6			
Boltzmann const k (dBJ/K)	−228.6			
A/D conversion and baseband processing loss (dB)	2			
Symbol rate (bps)	500			
	Vehicle	Geodetic	Hand-held	Portable
Typical G/T of revivers (dB/K)	≤−30.7	≤−32.7	≤−32.7	≤−33.9
Effective $C/N_0$ (dB-Hz)	33.4	31.4	31.4	30.2
Minimum coding gain requirements (dB)	4.2	6.2	6.2	7.4

The relationship between  $E_b/N_0$  and the carrier-to-noise ratio  $C/N_0$  is expressed as

$$E_b/N_0 = C/N_0 \cdot T_b, \quad (3)$$

where  $T_b$  is the data rate.

According to Equations (2) and (3), the corresponding values of  $P_e$ ,  $E_b/N_0$ , and  $C/N_0$  for  $T_b = 500$  bps can be calculated, as shown in Table 10.

BER is an index that measures the accuracy of data transmission within a specified period of time. The broadcast rate of the PPP service is usually high, so a large BER will cause frequent errors in the message, which will affect the user experience. Therefore, to ensure the user experience, the design BER requirement of the BDS PPP service is less than  $10^{-6}$ . According to Table 10, when the data rate is 500 bps and the BER is less than  $10^{-6}$ , the corresponding threshold of  $C/N_0$  is 37.6 dB. Therefore, the minimum coding gain requirement under the above conditions can be calculated by taking the typical G/T of receivers corresponding to the observation elevation angle of  $5^\circ$  as the critical values, as shown in Table 11.

## 5.2 | Coding method

Each frame of the PPP-B2b\_I augmentation navigation message before error correction encoding has a length of 486 bits and contains the message type (6 bits), message data (456 bits), and CRC (24 bits). The coding scheme

adopts a 64-ary LDPC (162, 81) (Huang et al., 2017, 2019). Each code word symbol is composed of 6 bits and is defined in the GF ( $2^6$ ) domain with a primitive polynomial of  $p(x) = 1 + x + x^6$ . A vector representation (MSB first) is used to describe the mapping relationship between non-binary symbols and binary bits. The message length is equal to 81 code word symbols, that is, 486 bits. The check matrix is a sparse matrix  $\mathbf{H}_{81,162}$  of 81 rows and 162 columns defined in the GF ( $2^6$ ) domain with the primitive polynomial of  $p(x) = 1 + x + x^6$ , of which the first  $81 \times 81$  corresponds to the information symbols and the last  $81 \times 81$  corresponds to the check symbols (Office China Satellite Navigation, 2019c).

The PPP-B2b\_I signal in the static scene was generated and broadcast by a satellite navigation signal simulator and received by a physical receiver for testing. The extended min-sum (EMS) algorithm was used to evaluate the decoding performance of the 64-ary LDPC (162, 81). The result is shown in Figure 8. If the value of the BER is  $10^{-6}$ , the corresponding coding gain is 7.5 dB (the difference between  $E_b/N_0$  after decoding and before decoding), which meets the minimum gain requirement shown in Table 11.

## 6 | SERVICE PERFORMANCE SIMULATION AND TESTING

The BDS PPP service is currently in the internal testing phase, and only the BDS constellation has been augmented temporarily. Section 6.1 presents the signal quality test

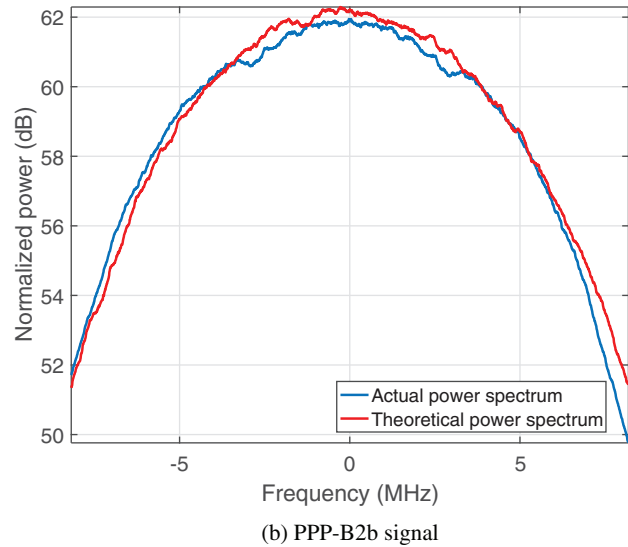
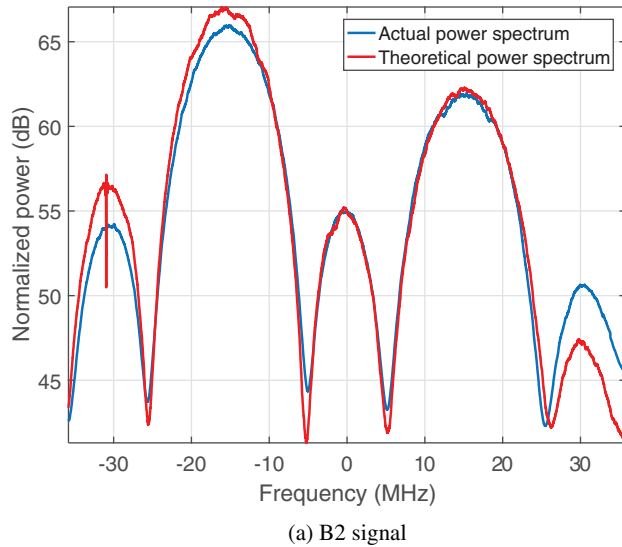


**FIGURE 9** Power spectrum of GEO-1 [Color figure can be viewed in the online issue, which is available at [wileyonlinelibrary.com](http://wileyonlinelibrary.com) and [www.ion.org](http://www.ion.org)]

results of PPP-B2b broadcast by the BDS-3 GEO-1 satellite in orbit and an actual user ground reception case. The preliminary results and performance analysis of the service based on the BDS constellation, which indicate that, at its current stage of development, the service has satisfactory capabilities, are provided in Section 6.2.

## 6.1 | Signal testing and evaluation

In order to investigate the signal quality and RF characteristics of the multiplexing PPP-B2b signal, a signal quality testing is carried out in Section 6.1.1, and an actual user ground reception case is presented in Section 6.1.2.

### 6.1.1 | Signal quality testing

On March 17, 2020, the signal broadcast by the GEO-1 satellite of BDS-3 was continuously observed with a 40 m L-band antenna of the Haoping Observatory of the National Time Service Center (NTSC) of the Chinese Academy of Sciences, and the quality of the signal was analyzed and evaluated.

The power spectrum of the B2 signal and its PPP-B2b component is shown in Figure 9. For the reference bandwidth, the power spectrum curves of the synthesized signal and the theoretical signal are in good agreement, and the deviation between them is only 0.26 dB.

Figure 10 shows the correlation function when PPP-B2b is independently received. It can be seen that the actual correlation curve is in good agreement with the theoretical

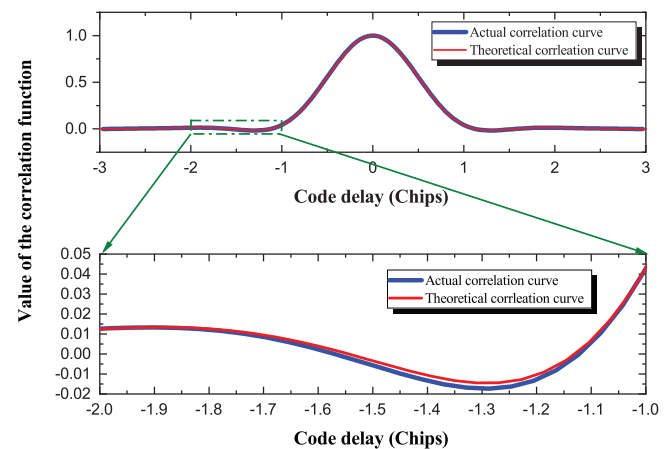


**FIGURE 10** Correlation function of PPP-B2b when it is independently received [Color figure can be viewed in the online issue, which is available at [wileyonlinelibrary.com](http://wileyonlinelibrary.com) and [www.ion.org](http://www.ion.org)]

correlation curve, and the impact of the correlation loss on the service can be ignored.

The S-curve bias (SCB) of the delay lock loop (DLL) discriminator of PPP-B2b with the main lobe receiving bandwidth is shown in Figure 11, in which its maximum value is only 0.0165 ns.

Figure 12 shows the actual baseband signal waveform of PPP-B2b. Statistics reveal that the average length difference between the positive-negative chip and the ideal chip is 0.002 ns and the standard deviation is 2.973 ns, which indicates that PPP-B2b has a good and stable signal waveform structure.

Finally, Figure 13 shows the consistency of the code and carrier phase of PPP-B2b. Statistical analysis reveals that the coherence between the code and the carrier of the



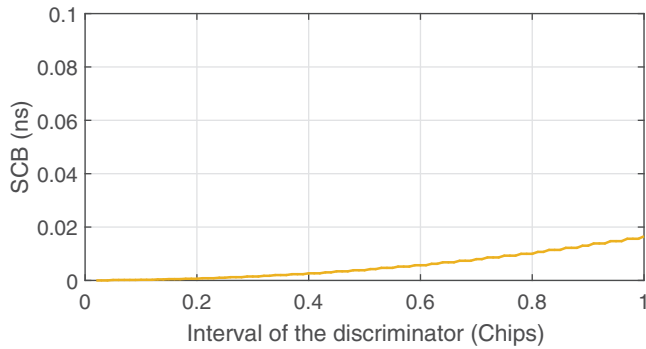


**FIGURE 11** SCB of DLL discriminator of PPP-B2b [Color figure can be viewed in the online issue, which is available at [wileyonlinelibrary.com](http://wileyonlinelibrary.com) and [www.ion.org](http://www.ion.org)]

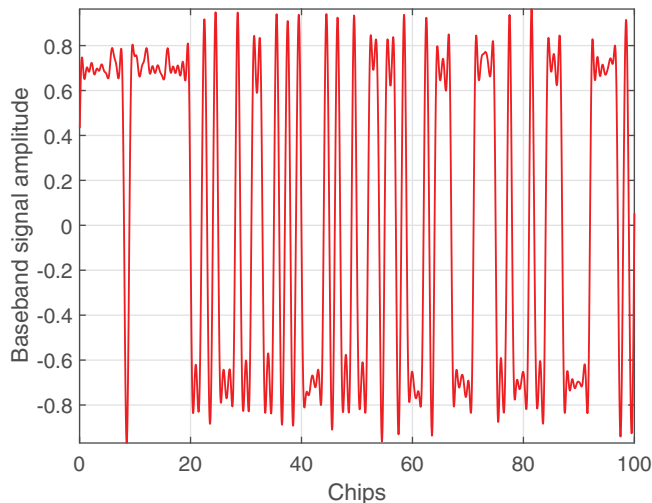


**FIGURE 12** Baseband signal waveform of PPP-B2b [Color figure can be viewed in the online issue, which is available at [wileyonlinelibrary.com](http://wileyonlinelibrary.com) and [www.ion.org](http://www.ion.org)]

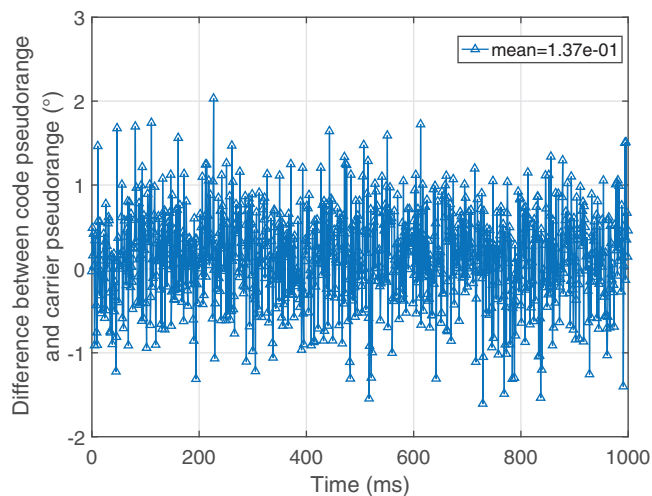


**FIGURE 13** Code and carrier phase consistency of PPP-B2b [Color figure can be viewed in the online issue, which is available at [wileyonlinelibrary.com](http://wileyonlinelibrary.com) and [www.ion.org](http://www.ion.org)]

**TABLE 12** Antenna specifications

Items	Specification
Working frequency	1190 MHz~1270 MHz
	1521 MHz~1615 MHz
Support positioning signal	GPS L1/L2
	GLONASS G1/G2/G3
	BDS B1/B2/B3
	Galileo E1/E5b
Phase center deviation	$\leq 2.0$ mm
Phase center repeatability	$\leq 1.0$ mm
Polarization	Right-handed circular polarization (RHCP)
Low noise amplification (LNA)	$43 \pm 2$ dB (Typical value)

signal is only  $0.137^\circ$ , which indicates a high degree of consistency.

### 6.1.2 | User reception testing

An external GNSS measurement antenna was used to receive the PPP-B2b signal in an open environment in Beijing (see the specifications of the antenna in Table 12). The received  $C/N_0$  and its statistics are shown in Figure 14. It can be seen that the typical received  $C/N_0$  of PPP-B2b is above 45.5 dB and the average value is approximately 47 dB, which meets the coding gain requirements in Table 11.

## 6.2 | Preliminary service performance

From April 15 to April 21, 2020, a static positioning experiment of the BDS PPP service was continuously performed in several cities in China. Currently, the service only augments a single BDS constellation. In the future, additional GNSS constellations will be augmented to further improve performance.

The convergence time is defined as the minimal time required for the position error to reduce to less than a certain value (0.3 m in the horizontal direction and 0.6 m in the vertical direction) and last at least 30 min, and the positioning accuracy is a measure of the position error statistics from the moment of convergence until the positioning work is over. They were both evaluated every two hours in the experiment, and the uncertainty of the accuracy was calculated by the root mean square (RMS) value of the positioning errors. By averaging the positioning accuracy and convergence time of each two-hour period, the average positioning accuracy and average convergence time can be obtained, as shown in Figure 15. It can be seen that the

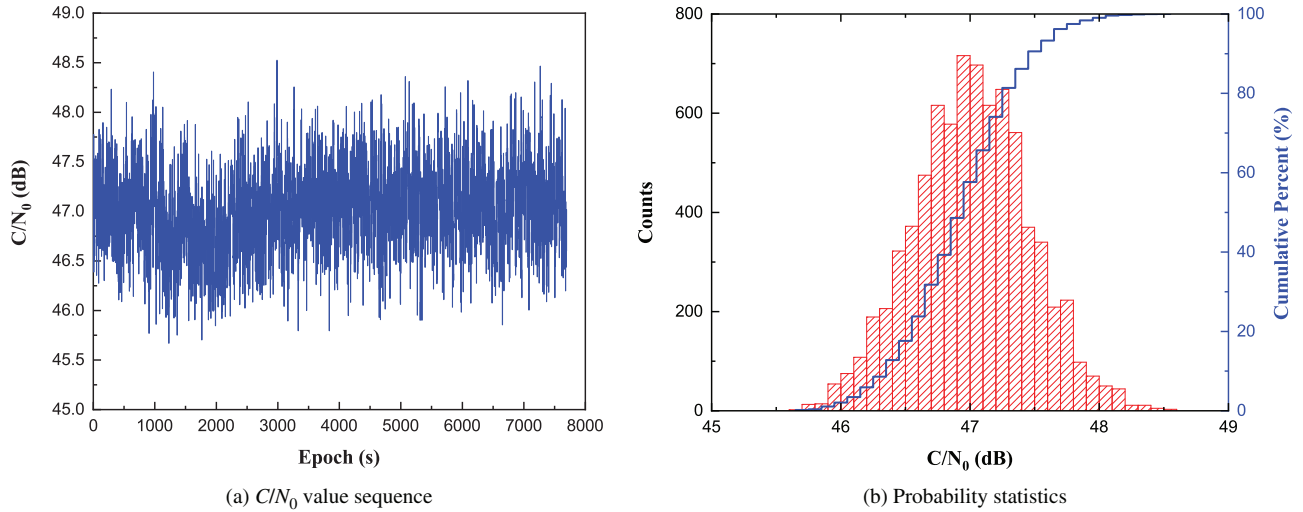


FIGURE 14  $C/N_0$  of PPP-B2b [Color figure can be viewed in the online issue, which is available at wileyonlinelibrary.com and www.ion.org]

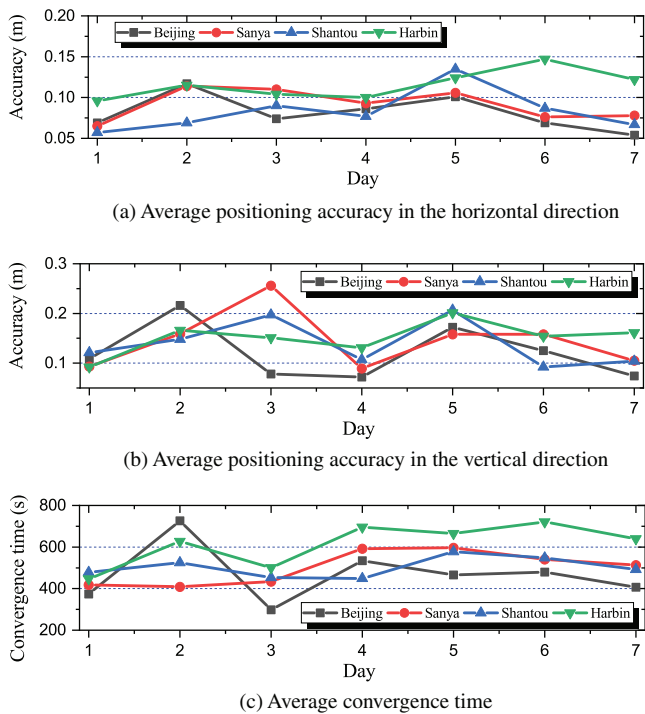


FIGURE 15 Average positioning accuracy and convergence time in static experiment at four different stations [Color figure can be viewed in the online issue, which is available at wileyonlinelibrary.com and www.ion.org]

service has good stability during the test. The average positioning accuracy of each station in the horizontal and vertical directions of each day is better than 0.15 m (RMS) and 0.3 m (RMS), respectively, and the average convergence time of each day does not exceed 800 s (about 13.3 min), which meets the design performance specifications. The

TABLE 13 The statistical results of the 7-day static positioning experiment

Stations	Accuracy (RMS,m)		Convergence time (s)
	Horizontal	Vertical	
Beijing	0.081	0.121	470
Sanya	0.092	0.145	501
Shantou	0.083	0.139	504
Harbin	0.115	0.151	614

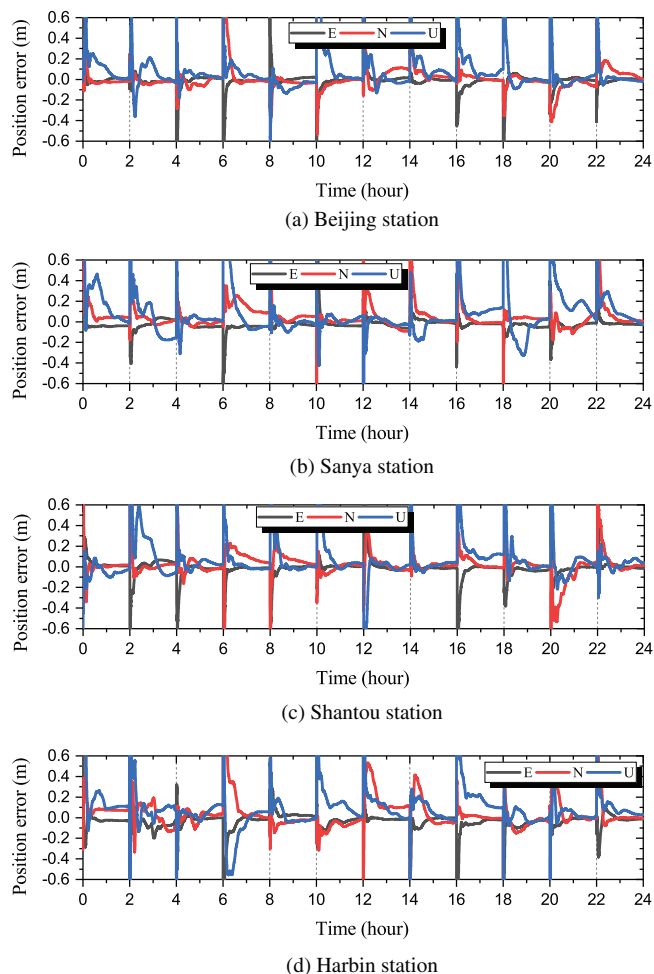
statistical results of the complete seven-day static positioning experiment are shown in Table 13.

Figure 16 presents the experimental results obtained on April 20, 2020, which indicate the position errors along the north (N), east (E), and up (U) axes of a ENU local-level frame (LLF), respectively.

## 7 | CONCLUSIONS

As one of the seven kinds of BDS-3 open services, PPP is of great significance for improving the service capability of BDS in high-precision fields. The BDS PPP service is designed and optimized based on BDS-3 and is committed to achieving high quality and performance with minimal system and resource costs.

This paper presents the design and implementation work of the BDS PPP service. The scheme design of the PPP-B2b signal is illustrated, which is constructed based on the optimized ACE-BOC multiplexing modulation method. By studying the key to the PPP augmentation navigation messages, the customized message format of the service, which can augment all visible satellites of the



**FIGURE 16** Position errors in static experiment at four different stations on April 20, 2020 [Color figure can be viewed in the online issue, which is available at [wileyonlinelibrary.com](http://wileyonlinelibrary.com) and [www.ion.org](http://www.ion.org)]

four core constellations in mainland China, is formulated. The LPDC coding method is used for the service, and an actual receiving testing result, which proves its high gain and effectiveness, is provided. Currently, the service has completed the first stage of design and is in the internal testing phase. The signal quality testing shows that the PPP-B2b signal has good RF characteristics; furthermore, the performance evaluation to date reveals that the positioning accuracy in the horizontal and vertical directions based on the single BDS constellation is better than 0.15 m and 0.3 m, respectively, and the average convergence time does not exceed 800 s, which meets the design performance specifications. The testing and evaluation results prove the effectiveness of the design and indicate that the service, at its current stage of development, has satisfactory capabilities.

After completion of the internal testing, BDS will formulate and release its PPP PS document and provide a free

high-precision PPP service to users in China and its surrounding areas. It is believed that, with the future augmentation of other GNSS constellations, the performance of the BDS PPP service will be further improved.

## ACKNOWLEDGMENTS

We extend our sincere gratitude to Ms. Jiang Nan and Dr. Li Fang for their help in proofreading and drawing.

## FINANCIAL DISCLOSURE

This study was supported by the National Natural Science Foundation of China (Grant Nos. 41974041, 61601009, and 61771272) and the Young Talent Supporting Program of the China Association for Science and Technology (Grant No. 2019QNRC001).

## CONFLICT OF INTEREST

The authors declare no potential conflict of interests.

## ORCID

Cheng Liu  <https://orcid.org/0000-0002-2861-5299>

Zheng Yao  <https://orcid.org/0000-0002-7657-644X>

## REFERENCES

- Cabinet Office. (2018a). *Quasi-Zenith satellite system performance standard (PS-QZSS-001)*. <https://qzss.go.jp/en/technical/download/pdf/ps-is-qzss/ps-qzss-001.pdf>
- Cabinet Office. (2018b). *Quasi-Zenith satellite system interface specification centimeter level augmentation service (IS-QZSS-L6-001)*. <https://qzss.go.jp/en/technical/download/pdf/ps-is-qzss/is-qzss-l6-001.pdf>
- Hadas, T., & Bosy, J. (2014). IGS RTS precise orbits and clocks verification and quality degradation over time. *GPS Solutions*, 19(1), 93–105. <https://doi.org/10.1007/s10291-014-0369-5>
- Hayes, D. (2018). *Galileo programme UPI-date*. [Presentation] Wyndham Grand Xi'an South Hotel, 5th November.
- Hayes, D., & Hahn, J. (2019). *2019-Galileo programme update*. [Presentation] ITC Gardenia Hotel, December.
- Héroux P. & Kouba J. (2001). GPS precise point positioning using IGS orbit products. *Physics and Chemistry of the Earth, Part A: Solid Earth and Geodesy*, 26(6-8), 573–578. [https://doi.org/10.1016/S1464-1895\(01\)00103-X](https://doi.org/10.1016/S1464-1895(01)00103-X)
- Huang, Q., Song, L., & Wang, Z. (2017). Set message-passing decoding algorithms for regular non-binary LDPC codes. *IEEE Transactions on Communications*, 65(12), 5110–5122. <https://doi.org/10.1109/TCOMM.2017.2746101>
- Huang, Q., Zhang, M., Wang, Z., & Zhang, X. (2019). FEC design for remote control and data transmission of aeronautic and astronautic vehicles. *Chinese Journal of Aeronautics*, 32(1), 159–166. <https://doi.org/10.1016/j.cja.2018.03.013>
- International Civil Aviation Organization (ICAO). (2018). *DFMC SBAS SARPs: Part A version 2.2 (Working Paper)*. [https://www.icao.int/airnavigation/Documents/NSP5\\_Report%20on%20Agenda%20Item%202.APPENDIX%20A1%20-%20DFMC%20SBAS%20SARPs%20Part%20A.pdf](https://www.icao.int/airnavigation/Documents/NSP5_Report%20on%20Agenda%20Item%202.APPENDIX%20A1%20-%20DFMC%20SBAS%20SARPs%20Part%20A.pdf)

- IWG SBAS. (2016a). *Satellite-based augmentation system dual-frequency multi-constellation definition document*. 31th SBAS IWG, Dakar, Senegal.
- IWG SBAS. (2016b). *Satellite-based augmentation system dual-frequency multi-constellation interface control*. 31th SBAS IWG, Dakar, Senegal.
- Kazmierski, K., Sośnica, K., & Hadas, T. (2017). Quality assessment of multi-GNSS orbits and clocks for real-time precise point positioning. *GPS Solutions*, 22(1). <https://doi.org/10.1007/s10291-017-0678-6>
- Office China Satellite Navigation. (2019a). *Development of the BeiDou navigation satellite system* (Version 4.0). <http://en.beidou.gov.cn>
- Office China Satellite Navigation. (2019b). *The application service architecture of BeiDou navigation satellite system* (Version 1.0). <http://en.beidou.gov.cn>
- Office China Satellite Navigation. (2019c). *BeiDou navigation satellite system signal: Space interface control document open service signal PPP-B2b* (Beta Version). <http://en.beidou.gov.cn>
- Office China Satellite Navigation. (2019d). *BeiDou navigation satellite system signal: Space interface control document open service signal B2b* (Beta Version). <http://en.beidou.gov.cn>
- Quasi-Zenith Satellite System (QZSS). (2018). *Centimeter Level Augmentation Service (CLAS)*. [https://qzss.go.jp/en/overview/services/sv06\\_clas.html](https://qzss.go.jp/en/overview/services/sv06_clas.html)
- Revnivykh, I. (2019). *GLONASS and SDCM status and development*. [Presentation] ITC Gardenia Hotel, December.
- RTCM Special Committee. (2013). *Differential GNSS (global navigation satellite systems) services: Version 3* (RTCM Standard 10403.2). [https://global.ihs.com/doc\\_detail.cfm?document\\_name=RTCM%2010403%2E2&item\\_s\\_key=00619725#product-details-list](https://global.ihs.com/doc_detail.cfm?document_name=RTCM%2010403%2E2&item_s_key=00619725#product-details-list)
- Yang, Y., Gao, W., Guo, S., Mao, Y., & Yang, Y. (2019). Introduction to BeiDou-3 navigation satellite system. *NAVIGATION*, 66(1), 7–18. <https://doi.org/10.1002/navi.291>
- Yao, Z., Guo, F., Ma, J., & Lu, M. (2017). Orthogonality-based generalized multicarrier constant envelope multiplexing for DSSS signals. *IEEE Transactions on Aerospace and Electronic Systems*, 53(4), 1685–1698. <https://doi.org/10.1109/TAES.2017.2671580>
- Yao, Z., Zhang, J., & Lu, M. (2016). ACE-BOC: Dual-frequency constant envelope multiplexing for satellite navigation. *IEEE Transactions on Aerospace and Electronic Systems*, 52(1), 466–485. <https://doi.org/10.1109/TAES.2015.140607>

**How to cite this article:** Liu C, Gao W, Liu T, Wang D, Yao Z, Gao Y, Nie X, Wang W, Li D, Zhang W, Wang D, Rao Y. Design and implementation of a BDS precise point positioning service. *NAVIGATION*. 2020;67:875–891. <https://doi.org/10.1002/navi.392>